A Systematic Analysis of Peptide Linker Length and Liposomal Polyethylene Glycol Coating on Cellular Uptake of Peptide-Targeted Liposomes

Jared F. Stefanick,[†] Jonathan D. Ashley,[†] Tanyel Kiziltepe,[†,§,*] and Basar Bilgicer[†,‡,§,*]

[†]Department of Chemical and Biomolecular Engineering, [‡]Department of Chemistry and Biochemistry, and [§]Advanced Diagnostics and Therapeutics, University of Notre Dame, Notre Dame, Indiana 46556, United States

ABSTRACT PEGylated liposomes are attractive pharmaceutical nanocarriers; however, literature reports of ligand-targeted nanoparticles have not consistently shown successful results. Here, we employed a multifaceted synthetic strategy to prepare peptide-targeted liposomal nanoparticles with high purity, reproducibility, and precisely controlled stoichiometry of functionalities to evaluate the role of liposomal PEG coating, peptide EG-linker length, and peptide valency on cellular uptake in a systematic manner. We analyzed these parameters in two distinct disease models where the liposomes were functionalized with either HER2- or VLA-4-antagonistic peptides to target HER2-overexpressing breast cancer cells or VLA-4-overexpressing myeloma cells, respectively. When targeting peptides were tethered to nanoparticles with an EG45 (~PEG2000) linker in a manner similar to a more traditional formulation, their cellular uptake was not enhanced compared to non-targeted versions regardless of the liposomal PEG coating used. Conversely, reduction of the liposomal PEG to PEG350 and the peptide linker to EG12 dramatically enhanced cellular uptake by ~9 fold and ~100 fold in the breast cancer and multiple myeloma cells, respectively. Uptake efficiency reached a maximum and a plateau with ~2% peptide density in both disease models. Taken together, these results demonstrate the significance of using the right design elements such as the appropriate peptide EG-linker length in coordination with the appropriate liposomal PEG coating and optimal ligand density in efficient cellular uptake of liposomal nanoparticles.

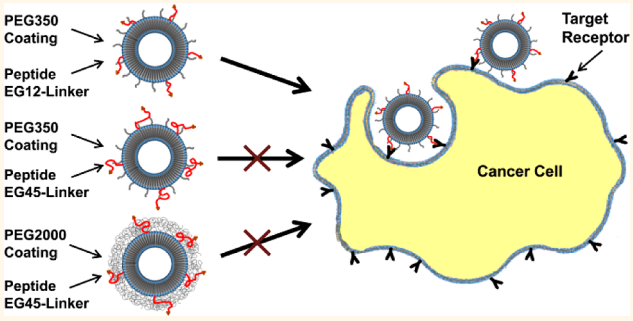

KEYWORDS: ligand-targeted liposome · polyethylene glycol · HER2 · VLA-4 · peptide-targeted liposome · peptide linker · cellular uptake

Polyethylene glycol (PEG) coated liposomal nanoparticles of a defined size range of 100 to 200 nm are efficient drug delivery systems since they combine increased stability, high circulation times, increased tumor accumulation, and decreased systemic toxicity.[1−5] Despite these particular advantages liposomal nanoparticles provide when compared to small molecule drugs, lack of selectivity for cancer cells still remains a major problem.[6] An important feature of liposomal nanoparticles is that they present particularly attractive scaffolds for the display of multiple functional groups on their surfaces. To overcome the selectivity problem, many researchers have taken the approach of active targeting by conjugating targeting ligands such as antibodies, antibody fragments, small molecules, and targeting peptides to improve the tumor targeting and cellular uptake of nanoparticle-based drug carriers.[7−14] However, active targeting of nanoparticles has not consistently shown successful outcomes.[15−17] At present, there is still an extensive debate on the relative contributions of active *versus* passive targeting in nanoparticle-based drug delivery systems.[18−24] The apparent discrepancy observed in the field of targeted liposomal nanoparticles has in part been attributed to differences in type of tumor models, however, most likely it originates from the PEG coatings of the particles, linkers used to conjugate the targeting ligands, as well as the different types of targeting ligands.

* Address correspondence to bbilgicer@nd.edu, tkiziltepe@nd.edu.

Received for review December 7, 2012 and accepted February 19, 2013.

Published online February 19, 2013
10.1021/nn305663e

On liposomal nanoparticles, PEG serves two functions: (i) to provide stealth to the particles for increased circulation time and (ii) to act as a linker to connect the targeting ligand to the particle. The current clinical and research standard for establishing optimal *in vivo* circulation enhancement is the incorporation of a 5 mol percent methoxy-PEG2000-DSPE (PEG2000; a mean of ~45 repeating units of ethylene glycol: EG45) in the liposome formulation.[2,25] This polymer length and percentage provides a complete PEG coating of the liposome surface while maintaining particle stability. PEG2000 has also been used as a linker to conjugate targeting ligands.[3,26] In certain particle designs, use of a longer linker such as PEG3350 or PEG5000 has been preferred presumably because longer linkers may present the targeting ligand above the PEG coating more effectively.[3,27−29] However, it is well established that long PEG polymers including PEG2000, PEG3350, and PEG5000 do not have a linear conformation in water.[30,31] Rather, they fold into a mushroom like globular structure,[32,33] burying a large fraction of the conjugated ligand into the PEG coating and sterically hindering the association of the ligand-targeted liposome with its target receptor. Although PEG itself has been determined to be an ideal molecule to enhance bioavailability of liposomal nanoparticles, the use of PEG2000 specifically as a liposomal coating and linker has been, in part, due to traditional reasons rather than scientific reasoning. Several reports in literature demonstrate that similar bioavailability profiles and *in vivo* circulation half-life can be achieved with much shorter liposomal PEG molecules such as PEG350, PEG550, and PEG750, despite the estimated PEG coverage of < 100%.[30,31] Furthermore, a shorter peptide linker may provide a more favorable thermodynamic receptor−ligand interaction. Although enthalpic parameters would remain the same regardless of linker length, a short linker would restrict the translational and conformational freedom of the peptide, reducing the overall entropic loss when the liposome binds to the cell. These provide a strong scientific rationale to evaluate the effect of shorter peptide linker lengths, in coordination with various liposomal PEG coatings, on tumor cell targeting and uptake.

In studies to date, the most common method of generating ligand-targeted nanoparticles involves coupling targeting elements directly to preformed nanoparticles as a second step following the preparation of the nanoparticles.[3,8,34−37] However, this approach results in significant variations in coupling yields and decreases binding activity due to side reactions that can yield chemical and conformational changes to the ligand.[38−41] This process causes batch-to-batch variations in ligand-targeted nanoparticle preparation and results in highly heterogeneous nanoparticle populations with inconsistent outcomes in cellular uptake and tumor targeting. In this study, we employed a multifaceted synthetic strategy where the targeting ligand is synthesized as a lipid conjugate and subsequently purified prior to nanoparticle preparation. The liposomal components are then mixed at desired ratios during nanoparticle preparation, a procedure that yields highly reproducible results with high purity and precisely controlled stoichiometric loading of targeting ligands. The precision and purity of nanoparticles prepared with this method enables the study of the effects of liposomal PEG coating, peptide linker length, and peptide density on cellular uptake in a systematic manner, without other compounding factors. In particular, by using well-characterized liposomes, we evaluated in detail the effect of these parameters on cellular uptake by Human Epidermal Growth Factor Receptor 2 (HER2) overexpressing breast cancer cells. HER2 is overexpressed in 25% of breast cancer cases and is associated with poor prognosis making it an ideal receptor to target this disease.[42,43] In our approach, we used a short cyclic-peptide antagonist of HER2 as the targeting ligand and identified the optimal design elements for maximum cellular uptake. We then validated our findings by applying and evaluating the optimized design elements in a Very Late Antigen-4 (VLA-4) overexpressing multiple myeloma model. In both disease models, we consistently demonstrated that cellular uptake is significantly enhanced when a shorter peptide linker such as EG12 was used in combination with PEG350 liposomal coating instead of the industry standard PEG2000. These results established the significance of using the right design elements, such as the appropriate peptide EG-linker length in coordination with the appropriate liposomal PEG coating and optimal ligand density in efficient targeting of tumors.

RESULTS AND DISCUSSION

Validation of the Selective Binding of a HER2-Antagonist Peptide to HER2-Overexpressing Breast Cancer Cells. It is well established that HER2 is overexpressed in 25% of breast cancer cases, and there are several HER2-overexpressing breast cancer cell lines, including BT-474 and SK-BR-3, that provide useful tools to evaluate and optimize HER2-targeted liposomal nanoparticles. We validated HER2 expression in these cell lines in a flow cytometry assay by using an anti-HER2 primary antibody followed by a fluorescein-labeled secondary antibody. HER2 expression levels were consistent with values previously reported in literature,[44] with both the BT-474 and SK-BR-3 cell lines overexpressing HER2 in significant quantities (Figure 1A). The MCF7 breast cancer cell line was used as a negative control with very low levels of HER2 expression.

In our approach, to target HER2-overexpressing cells, we used a short cyclic-peptide sequence as the targeting ligand for the various advantages provided over the use of conventional antibody macromolecules (or their fragments) including ease of preparation,

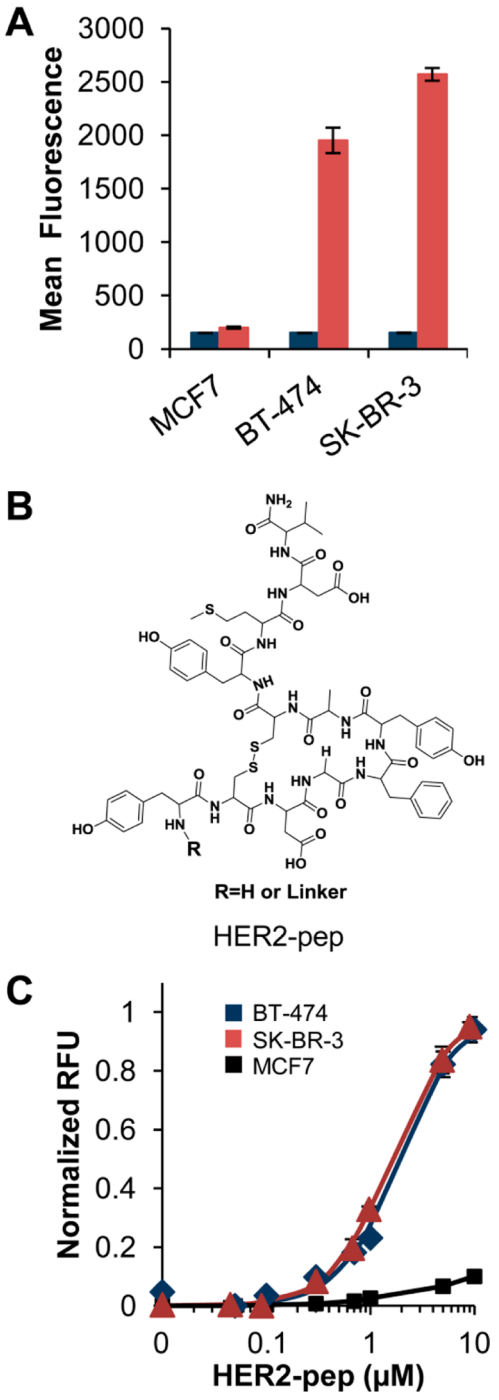

Figure 1. HER2 expression in breast cancer cells and identification of a HER2-antagonist peptide. (A) HER2 expression levels in MCF7, BT-474, and SK-BR-3 were determined in a flow cytometry assay using a primary anti-HER2 antibody followed by a fluorescein labeled secondary antibody (red columns). Isotype controls are shown as blue columns. (B) Structure of HER2-antagonist peptide (HER2-pep) is shown. (C) Cellular binding assays were performed using fluorescein labeled HER2-pep and binding to BT-474 (blue), SK-BR-3 (red), and MCF7 (black) was detected by flow cytometry. Control experiments were performed with fluorescein-labeled nonspecific peptide and the background binding was subtracted for each data point. Fluorescence signal was normalized based on the highest and lowest observed values for the BT-474 and SK-BR-3 cell lines. All experiments were done in triplicate, and data represent means (±SD).

lower cost, lower antigenicity, decreased opsonization, and increased stability to degradation.[45−49] With a broad range of affinities, peptide targeted therapies can provide selectivity through multiple low to moderate affinity interactions.[50,51] Liposomes also provide excellent scaffolds for multivalent presentation of the peptide ligands, enhancing the binding avidity and selectivity for overexpressed receptors. The cyclic peptide sequence, YCDGFYACYMDV (HER2-pep; Figure 1B), was previously identified as a HER2-antagonist by Berezov *et al*. and has been reported to bind to an extracellular HER2 domain with submicromolar affinity (K_d = 150 nM).[52] We demonstrated selective binding of this peptide to SK-BR-3 and BT-474 cells in a cellular binding assay, where we incubated the cells on ice with a fluorescein-labeled version of this peptide and detected peptide binding using flow cytometry (Figure 1C). Control experiments performed with labeled nonspecific peptide showed only minimal background binding and was subtracted from each data point. HER2-pep demonstrated efficient and selective binding to both SK-BR-3 (K_d = 1.75 μM) and BT-474 (K_d = 1.97 μM) cell lines. Only minimal binding was observed to the MCF7 cells, consistent with the negligible levels of HER2 expression. It is noteworthy that we observed ∼10 fold weaker binding affinity in cellular binding assays compared to the binding reported for the recombinant HER2 protein.[52] This apparent difference most likely emerges from the steric and structural differences between the HER2 receptor that is overexpressed on the surface of cancer cells and the recombinantly expressed soluble HER2 protein that was used in the previous studies.

Development of a Multifaceted Synthetic Strategy for Preparation of Ligand-Targeted Liposomal Nanoparticles with Precisely Controlled Stoichiometry of Functionalities. In the most commonly employed methods to date, targeting ligands are coupled directly to preformed nanoparticles resulting in significant fluctuations in coupling yields, decreased ligand activity, surface heterogeneity, and substantial batch-to-batch variation.[38−41] To overcome these problems, we employed a multifaceted synthetic strategy in our approach, where we synthesized and purified the peptide−EG−lipid conjugates to >98% purity prior to nanoparticle preparation. This method of peptide incorporation has several advantages when compared to the postinsertion methods commonly used including precise control over the number of targeting ligands, elimination of variability in coupling yield, and elimination of decreased binding activity due to chemical side reactions. In addition, this strategy eliminates the need to purify the liposomes that are formed, ensuring maximal particle recovery. This approach results in highly homogeneous particle populations with high purity while minimizing batch-to-batch variability.

We performed the synthesis of the peptide−EG−lipid conjugates on a solid support, using standard Fmoc

chemistry protocols (Figure 2). Since the various peptide EG-linker lengths that were employed in this study had different chemical functionalities, two different synthetic strategies on the solid support were employed to create the desired products. The first synthetic strategy, described in Figure 2A, was used to conjugate DSPE-PEG2000-NH_2 to the targeting peptide which was synthesized on either the Rink amide or Wang resin. Following the last Fmoc protecting group removal, succinic anhydride was introduced to react with the free N-terminus to generate a carboxylic acid moiety at the distal end of the peptide. This carboxylic acid was activated with HBTU, which was followed by introduction of DSPE-PEG2000-NH_2 in DMF, and the reaction was run overnight. The resulting product was cleaved from the resin and purified *via* RP-HPLC. Peptide cyclization through disulfide bond formation was performed in DMF with DIEA at room temperature overnight and repurified. This approach dramatically increased the product yield (~20%) compared to a conjugation strategy where the carboxylic acid is positioned on the PEG2000 linker and is coupled to the amine terminus of the peptide, which practically yielded no product. Nevertheless, with the shorter EG linkers, the coupling yields for the reactions where the carboxylic acid terminus was on the EG was satisfactory (10−65% product yield), hence we followed a different synthetic approach (Figure 2B). As in the first strategy, the peptide was synthesized on a resin, followed by the coupling of an EG linker of a desired length. The EG linker contains a carboxylic acid moiety to couple to the amine containing peptide and a Fmoc protected amine functionality for continued synthesis. After removal of the Fmoc from the peptide coupled EG, a L-lysine residue is coupled to provide branching. Two fatty acyl chains are then coupled to both the α- and ε-amines to generate the hydrophobic tail of the molecule that will embed into the lipid bilayer of the liposomes. Palmitic acid was chosen in lieu of a conventional carboxylic acid terminated phospholipid, such as DPPE-GA, because of its greater chemical stability due to the lack of the phosphoester bond and increased solubility in typical solid phase reaction solvents such as DMF and DCM. The products were then cleaved from the resin and purified *via* RP-HPLC. Purity of the synthesized conjugates were characterized by analytical HPLC and mass spectrometry analysis, where we routinely achieved greater than 98% purity as demonstrated by the representative HPLC (Figure 2C) and MS peaks (Figure 2D) of EG12-conjugated HER2-pep. Mass spectrometry data and product yields of all synthesized peptide-EG-lipid conjugates are also provided (see Supporting Information, Table S1 and Figures S1−S15).

Liposomes were prepared using purified peptide−EG−lipid conjugates, PEG-DSPE, HSPC, and cholesterol, which were mixed to produce nanoparticles with the desired peptide linker length and liposomal PEG coating (Figure 2E). The components were mixed at specific stoichiometries to achieve precise control over the number of functional ligands on each particle, while maintaining reproducibility in nanoparticle production (see Supporting Information, Figure S16). Nanoparticles with varying liposomal PEG coating, varying peptide EG-linker length, and varying peptide densities were prepared to evaluate the effect of these parameters on cellular uptake and tumor targeting. The liposomes were sized *via* extrusion through a polycarbonate membrane to yield an average diameter of 100 nm as detected by dynamic light scattering (DLS) analysis (Figure 2F). Lissamine rhodamine B PE or fluorescein PE was incorporated into the liposomes for cellular uptake and imaging experiments. Regardless of liposomal formulation, including the addition of fluorescent imaging agents or targeting agents, the mean diameter of the particles remained constant (see Supporting Information, Table S2 for particle sizing and zeta potential measurements).

Effect of Liposomal PEG Coating on Cellular Uptake. The standard method for generating stealth nanoparticles for an increased *in vivo* circulation half-life is the incorporation of 5% PEG2000.[2,25] Literature reports suggest that for efficient active targeting, the length of the linker molecule has to be at least as long as the PEG coating.[3,27] Therefore, in targeted liposome preparations, attaching the targeting ligand onto the distal end of functionalized PEG molecules—that are of at least ~45 ethylene glycol units (EG45 ≈ PEG2000)—has become the standard for both academic and industrial research. However, it is well established that long PEG molecules do not have a linear conformation in water, but rather fold into a globular mushroom like structures,[32,33] possibly hindering the accessibility of the targeting ligand on the liposome surface. Furthermore, in our experiments performed with HER2-pep targeted liposomes, we observed no difference in the uptake of targeted (95:10:3:2 HSPC:CHOL:PEG2000:HER2-pep) or non-targeted (95:10:5 HSPC:CHOL:PEG2000) nanoparticles prepared by a PEG2000 liposomal coating and an EG45 or EG72 peptide linker, further supporting this hypothesis (Figure 3A). This prompted the question of whether the standard way of preparing targeted liposomes is optimal for maximal cellular targeting. Importantly, it has been demonstrated that 5% PEG350, PEG550, and PEG750 coatings, despite providing less than 100% surface coverage, can achieve similar circulation half-lives to 5% PEG2000 coating.[30,31] This provides a strong rationale to elucidate the effects of shorter liposomal PEG coating in coordination with shorter peptide linker lengths in tumor targeting.

In our approach, we first examined the effect of liposomal PEG coating while keeping the peptide linker length of EG45 constant (Figure 3B). Liposomal nanoparticles (100 nm) with varying PEG coatings were prepared. The liposomal PEG lengths chosen for the study include PEG350, PEG550, PEG750, PEG1000, and PEG2000, which correspond to mean EG repeat units of approximately 8, 12, 17, 22, and 45, respectively.

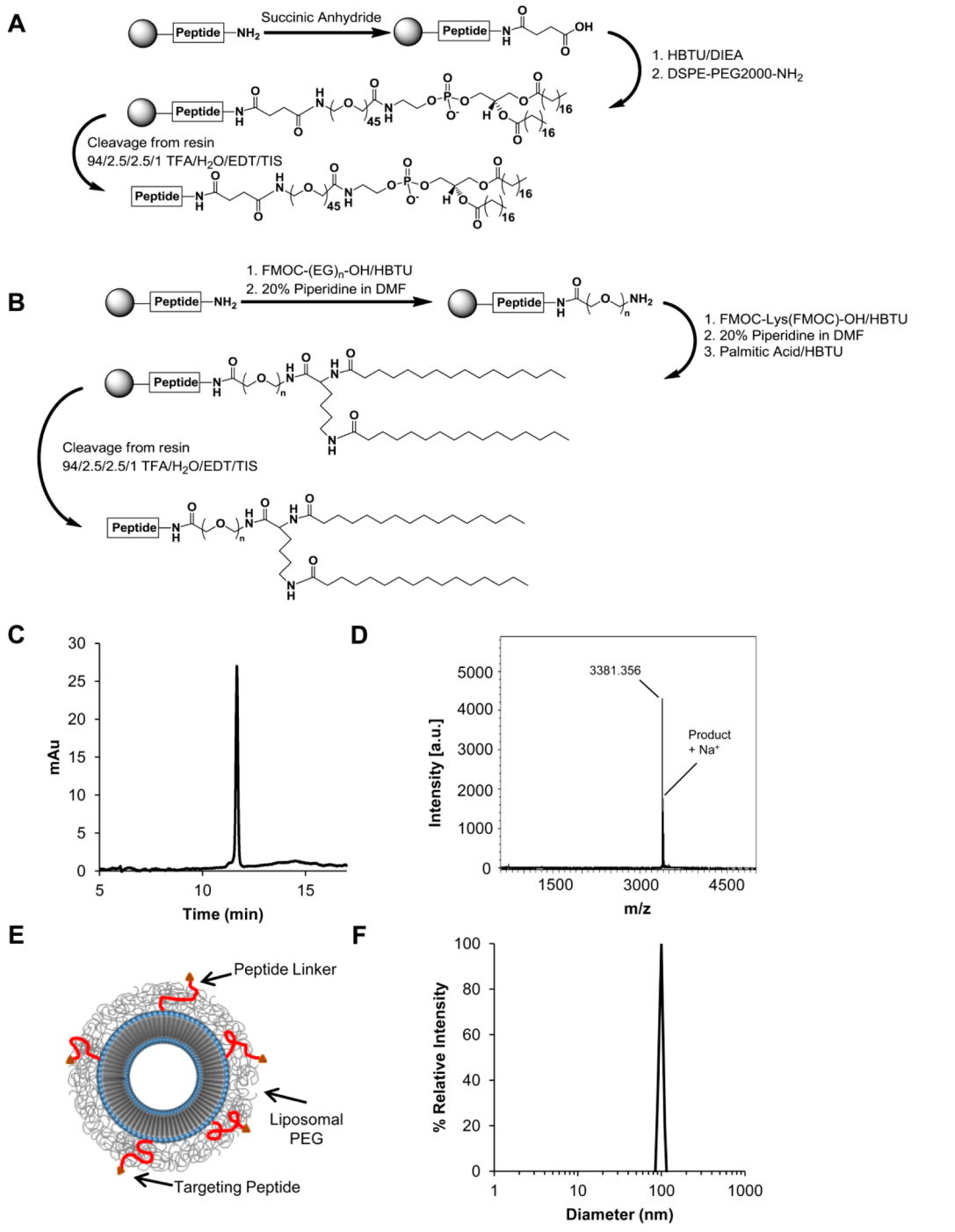

Figure 2. Synthesis and characterization of targeting peptide conjugated liposomes. (A) Schematic of the synthetic steps for peptide conjugation to DSPE-PEG2000-NH_2 (~45 EG units) using solid support. (B) Schematic of the synthesis of amphiphilic molecules with various peptide EG-linker lengths, including EG6, EG12, EG18, EG24, EG30, EG36, and EG72. (C) Representative RP-HPLC chromotograph of HER2-pep with EG12 peptide linker showing high purity of synthesized molecules. (D) Representative MALDI-MS spectrum of HER2-pep with EG12 linker. Expected mass, 3380.85; found mass, 3381.356. (E) Schematic of the synthesized ligand-targeted liposomes. (F) Dynamic light scattering analysis of nanoparticles.

Targeting liposomes were formulated with 95:10:3:2 HSPC:CHOL:PEGX-DSPE:HER2-pep-EG45-DSPE where X corresponds to the PEG molecular weights listed above. A non-targeted, non-PEGylated control liposome (100:10 HSPC:CHOL) was included in addition to non-targeted liposomes with variable liposomal PEG lengths (95:10:5 HSPC:CHOL:PEGX-DSPE). For cellular uptake studies, 0.2% fluorescein PE was added as a fluorescent marker and cellular uptake was quantitatively evaluated in HER2-overexpressing breast cancer cell lines using flow cytometry. To distinguish between nanoparticle association and uptake, cells were trypsinized before flow cytometric analysis. Interestingly, our flow cytometric analysis revealed that regardless of

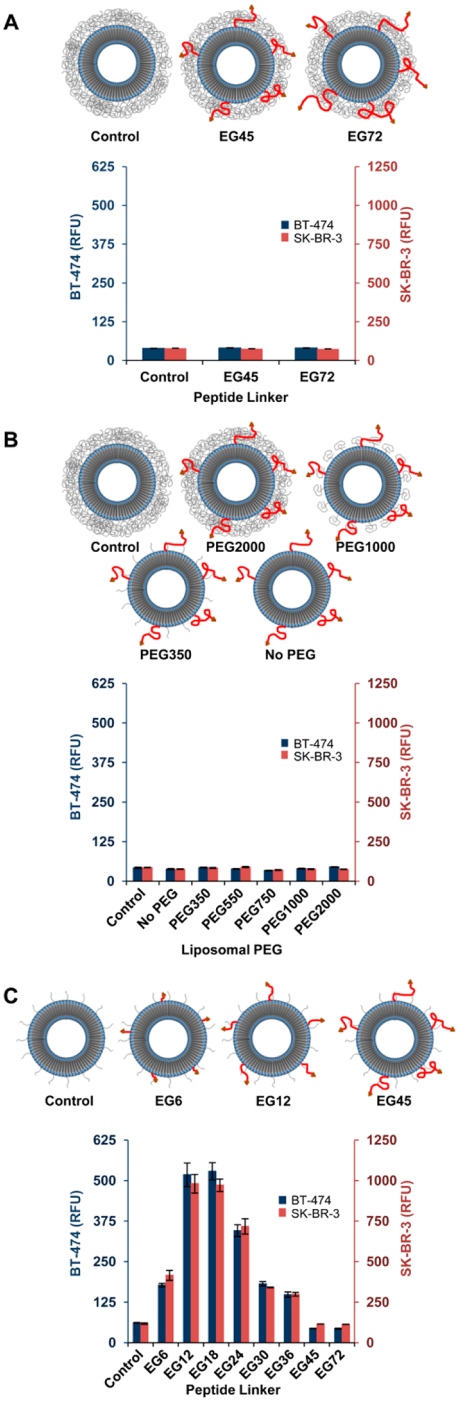

Figure 3. Effect of liposomal PEG coating and peptide EG-linker length on the cellular uptake of HER2-targeted liposomes. (A) Liposomes composed of PEG2000 liposomal coating with and without the EG45 or EG72 peptide linker were assayed for cellular uptake. (B) The effect of liposomal PEG length on the uptake of HER2 targeted liposomes with EG45 linker. The liposomal PEG lengths investigated include PEG350, PEG550, PEG750, PEG1000, and PEG2000. (C) The effect of peptide−EG−linker length on the uptake of liposomes with PEG350 liposomal coating. The peptide linker lengths investigated include EG6, EG12, EG18, EG24, EG30, EG36, EG45, and EG72. Non-targeted controls were also included. Cellular uptake by BT-474 cells (left *y*-axis; blue columns) and SK-BR-3 cells (right *y*-axis; red columns) were determined by flow cytometry. All experiments were done in triplicate, and data represent means (±SD).

liposomal PEG coating, there is no detectable enhancement in nanoparticle uptake with an EG45 linker, despite the addition of the HER2-pep targeting ligand (Figure 3B and Supporting Information Figure S17A for targeted formulations; Figure S17B for non-targeted formulations). This suggests that the EG45 peptide linker itself limited the availability of the peptide to bind to its respective receptor independent of the liposomal PEG coating. Given that EG45 linker does not preserve an extended linear structure in water, but rather folds into a globular mushroom like structure,[32,33] it is likely that the targeting peptides remain buried in the PEG cloud instead of being surface exposed, sterically hindering the association of the ligand with the target receptor. This led to our investigation into the effect of shorter ligand linker length to achieve enhanced cellular uptake.

Evaluation of Peptide EG-Linker Length on Uptake. Owing to the success of PEG2000 in increasing liposome bioavailability *in vivo*, little work has been performed in evaluating shorter peptide EG-linker length in coordination with shorter liposomal PEG coatings in effective targeting. Because PEG lengths as short as PEG350 have been shown to elicit similar plasma circulation lifetimes as PEG2000,[30,31] we evaluated if active targeting and cellular uptake can be enhanced by using liposomes with 5% PEG350 coating. We predicted that the use of PEG350 as the liposomal PEG will enable the use of shorter peptide EG-linker lengths to avoid the problems associated with EG45, yet still be longer than liposomal PEG350 coating to enable active targeting. Therefore, we formulated liposomes that incorporated PEG350 liposomal coating and HER2-pep conjugated lipids with varying linker lengths of EG6, EG12, EG18, EG24, EG30, EG36, EG45, and EG72 (Figure 3C). Targeted liposomes were formulated as 95:10:3:2 HSPC:CHOL:PEG350:HER2-pep with a nontargeted control (95:10:5 HSPC:CHOL:PEG350). Cellular uptake was evaluated with both BT-474 and SK-BR-3 cell lines. When EG6 linker was incorporated as the targeting element, there was minimal uptake presumably due to the peptide not being presented beyond the liposomal PEG coating. Alternatively, the linker may not provide enough length for the peptide to reach the binding pocket on the receptor. A remarkable enhancement in uptake was observed when using an EG12 linker (~9 fold greater than control). This trend continued for an EG18 linker, but gradually declined when EG24 linker was used and completely diminished with an EG45 and EG72 linker. Similar trends were observed at longer time points with the EG12 linker showing a ~5 fold and ~4 fold enhancement greater than control liposomes at 24 h for BT-474 and SK-BR-3, respectively (see Supporting Information, Figure S17C−E).

The dramatic enhancement observed with EG12 linker is likely due to a variety of factors. Tethering the peptide to a shorter linker restricts the translational and conformational freedom of the peptide, thereby

reducing the overall entropic loss when the liposome binds to the cell. Cellular binding experiments performed with targeting liposomes (95:10:3:2 HSPC:CHOL:PEG350:HER2-pep) containing either a EG12, EG24, or EG36 linker showed apparent K_d values in the order of $K_d^{EG12} < K_d^{EG24} < K_d^{EG36}$ for both BT-474 and SK-BR-3 cell lines (see Supporting Information, Figure S18A,B). This suggests that shortening the linkers to an optimal size does increase the avidity of the system which then facilitates binding and subsequent internalization. Furthermore, a shorter EG linker will adopt a more linear conformation, unlike a longer linker which will fold upon itself to form a globular, mushroom like structure. This decreased flexibility may also limit the nonspecific interactions of the peptide with the lipid bilayer.

It is also worthwhile to evaluate the effect of lipid tail content on uptake efficiency. To this end, we synthesized HER2-pep with an EG12 peptide linker and a variety of lipid tail designs including stearic acid, DPPE, DSPE, and DOPE to compare to the results with the palmitic acid tails. Targeted liposomes were formulated as 95:10:3:2 HSPC:CHOL:PEG350:HER2-pep with a non-targeted control consisting of 95:10:5 HSPC:CHOL:PEG350. Results show near identical results when stearic acid, DPPE, and DSPE are used as lipid tails in lieu of palmitic acid, but incorporation of DOPE decreased the uptake efficiency (see Supporting Information, Figure S19). These results suggest that provided that peptides are tethered to saturated lipid tails ≥16 carbons in length, the presence of the phospholipid does not adversely affect the accessibility of the peptide to bind or the net uptake of liposomes. However, the use of an unsaturated lipid (DOPE) decreased the uptake to approximately half of the observed values. This is likely due to the nonuniform packing of unsaturated lipid in the predominantly saturated lipid bilayer, which may affect the peptide presentation. It should be noted that due to our method for coupling traditional phospholipid molecules to peptides on the solid support, extra spacing is provided from the lipid anchor to the peptide due to the presence of succinic acid, ethanolamine, and phosphoester bond. Thus, net linker length will vary depending on synthetic method used and optimal EG linker length may shift to a slightly shorter length when phospholipids are used in place of fatty acyl chains. As an additional control experiment, we synthesized a PEGylated lipid with PEG350 and palmitic acid tails (PEG350-PA), incorporated the molecule into both non-targeted (95:10:5 HSPC:CHOL:PEG350) and liposomes targeted with HER2-pep conjugated to an EG12 linker (95:10:3:2 HSPC:CHOL:PEG350:HER2-pep-EG12-PA) and compared their efficacy to liposomes consisting of the commercially available PEG350-DSPE (see Supporting Information, Figure S20). The results show that incorporation of PEG350-PA does not change the behavior of either the targeting or non-targeting liposome relative to PEG350-DSPE. It is also noteworthy that the zeta potential did not differ significantly between samples (see Supporting Information, Table S2). Collectively, these results demonstrated that a shorter liposomal PEG coating than the standard PEG2000, in coordination with a shorter peptide EG-linker length than the standard EG45, provided much enhanced cellular targeting and uptake.

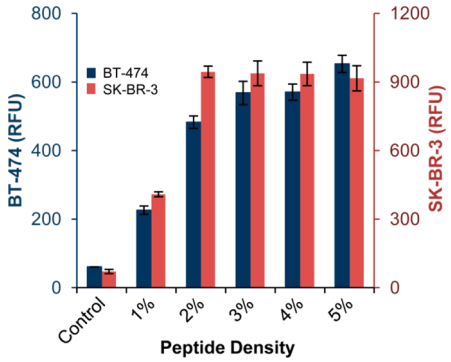

Figure 4. Effect of peptide density on the cellular uptake of HER2-targeted liposomes. Liposomes with PEG350 coating and EG12 peptide linker were prepared at the indicated HER2-pep densities. The valency of HER2-pep was varied between 0 and 5% of the total lipid. Cellular uptake by BT-474 cells (left *y*-axis; blue columns) and SK-BR-3 cells (right *y*-axis; red columns) were determined by flow cytometry. All experiments were done in triplicate, and data represents means (±SD).

It is noteworthy that some groups have established that increasing the linker length in PEG2000 based liposome designs increases the uptake of liposomes. For example, Gabizon *et al.* showed that the use of PEG3350 (~76 EG units) as a linker significantly out performs the PEG2000 counterpart in folate targeted therapies.[53] Yamada *et al.* published similar findings with the use of a PEG5000 (~113 EG units) linker.[29] However, these are special circumstances where the ligand in analysis possesses a very high affinity for the target receptor ($K_d \approx 1$ nM)[54] and multivalent interactions of the ligand with the cell surface receptors are likely not as essential compared to low-to-moderate affinity ligands. Similarly, when the targeting ligand is an antibody or antibody fragment, PEG2000 liposomal coating and PEG2000 linker may not cause a steric shielding problem since these targeting ligands are significantly larger (25−150 kDa) and readily water-soluble compared to some targeting peptides. Thus, while a PEG2000 liposomal coating and a linker length of PEG2000 or longer may provide promising outcomes when the targeting ligand has very high affinity for the receptor or larger biomolecules such as antibodies are used as targeting ligands, our results demonstrated that a finer design is imperative when working with smaller, low-to-moderate affinity ligands such as peptides.

Evaluation of Peptide Valency on Nanoparticle Uptake. Our multifaceted synthetic strategy allows precise control over the exact number of targeting ligands per

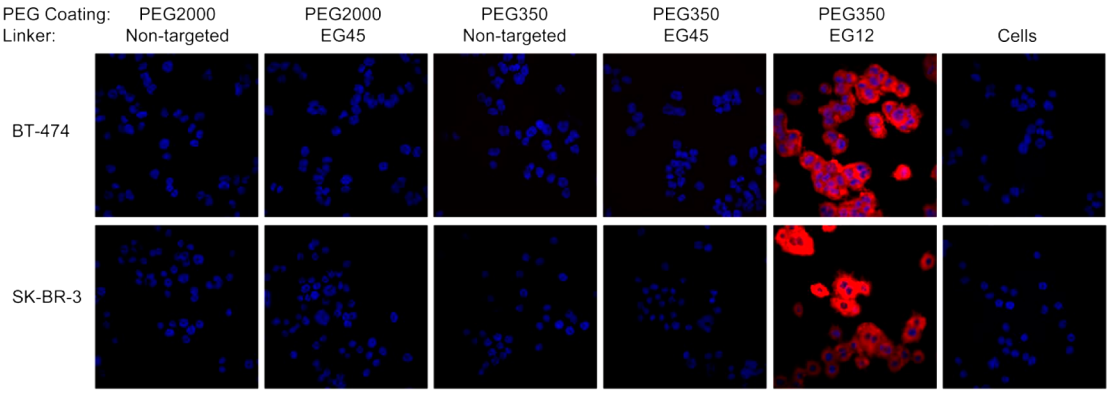

Figure 5. Determination of cellular uptake *via* confocal microscopy. Rhodamine-labeled liposomes with the indicated liposomal PEG coating and EG-linker were prepared and incubated with BT-474 (top) and SK-BR-3 (bottom) cell lines for 3 h at 37 °C. Non-targeted liposomes were included as controls. Internalization of nanoparticles was determined with a Nikon A1R confocal microscope using a 40× oil lens. Image acquisition was performed by Nikon Elements Ar software.

liposome. Therefore, we next examined the relationship between peptide valency and cellular uptake. We prepared liposomes with peptide densities of 0, 1, 2, 3, 4, and 5% of the total phospholipids (95:10:(5-*n*):*n* HSPC:CHOL:PEG350:HER2-pep-EG12-PA where $n = 0-5$) to find the optimal conditions for maximal uptake using PEG350 as the liposomal coating and EG12 as the peptide linker (Figure 4). For both the BT-474 and SK-BR-3 cell lines, the maximal uptake took place at ~2% and then reached a plateau. The observed plateau is likely due to the saturation of cellular surface receptors and the corresponding uptake mechanisms. Although these results establish 2% peptide density as the optimal density for maximum cellular uptake *in vitro*, this may not be directly transferable to *in vivo* studies. The high surface density of peptide on the liposome surface may accelerate clearance of the particles from blood circulation by opsonization and subsequent detection by the reticuloendothelial system (RES). Ongoing research is currently evaluating the effect of peptide valency in tumor targeting and uptake *in vivo*.

Validation of Cellular Uptake Results with Confocal Microscopy. While flow cytometry provides us with a powerful quantitative tool, it does not distinguish between cellular association and cellular internalization. To confirm cellular uptake and internalization of the nanoparticles by the HER2-overexpressing cells, confocal microscopy experiments were performed with rhodamine-labeled liposomes (95:10:5 HSPC:CHOL:PEGX-DSPE for control liposomes and 95:10:3:2 HSPC:CHOL:PEGX-DSPE:HER2-pep for targeted liposomes). In both the BT-474 and SK-BR-3 cell lines, efficient uptake was observed when PEG350 liposomal coating and EG12 peptide linker was used, confirming the results observed with flow cytometry experiments (Figure 5). As seen before, the use of EG45 as the peptide linker, regardless of either PEG350 or PEG2000 liposomal PEG, provided no enhancement in cellular uptake. Additional imaging experiments, using confocal microscopy, were performed by labeling intracellular acidic vesicles (endosomes/lysosomes) with LysoTracker Red and examining the colocalization of fluorescein labeled nanoparticles (95:10:5 HSPC:CHOL:PEG350 for the control liposome and 95:10:3:2 HSPC:CHOL:PEG350:HER2-pep-EG12-PA for the targeted liposome). Significant internalization into lysosomes was observed with the EG12 liposomal formulation in both cell lines, with no internalization evident with a non-targeted liposome (see Supporting Information, Figures S21 and S22).

Effect of Liposomal PEG Coating and EG Linker Length on Cellular Uptake in VLA-4 Overexpressing Multiple Myeloma Model. To confirm that the conclusions derived from the experiments presented with HER2-targeting liposomes can be applied broadly to other peptide targeted liposomal delivery systems, we have undertaken a similar analysis with VLA-4 overexpressing multiple myeloma cells. It has been demonstrated that multiple myeloma cell lines express the VLA-4 subunits and α_4- and β_1-integrins. First, we validated $\alpha_4\beta_1$ integrin expression in the NCI-H929 myeloma cell line (Figure 6A). Several antagonistic peptides of VLA-4 have been identified,[55−57] and the cyclic peptide sequence, YCDPC (VLA4-pep; Figure 6B), has been shown to bind to VLA-4 expressing myeloma cells with specificity.[58] We validated selective binding of VLA4-pep to NCI-H929 cells (Figure 6C) and prepared VLA-4 targeted liposomal nanoparticles with varying liposomal PEG coating and peptide EG-linker lengths. We then analyzed cellular uptake in NCI-H929 myeloma cells by flow cytometry and confocal microscopy. Our results obtained with myeloma cells demonstrated consistent results with the HER2 system. There was almost no enhancement in cellular uptake when PEG2000 coated liposomes (95:10:5 HSPC:CHOL:PEG2000 for control liposomes and 95:10:3:2 HSPC:CHOL:PEG2000:VLA4-pep for targeted liposomes) were used with EG45 or EG72 linkers (Figure 6D). However, liposomes prepared using PEG350 coating with the shorter EG12 linker (95:10:5 HSPC:CHOL:PEG350 for control liposomes and 95:10:3:2 HSPC:CHOL:PEG350:VLA4-pep-EG12-PA for targeted liposomes) showed a dramatic enhancement of cellular uptake reaching up to ~100 fold (Figure 6E). Similar to the HER2 system, uptake

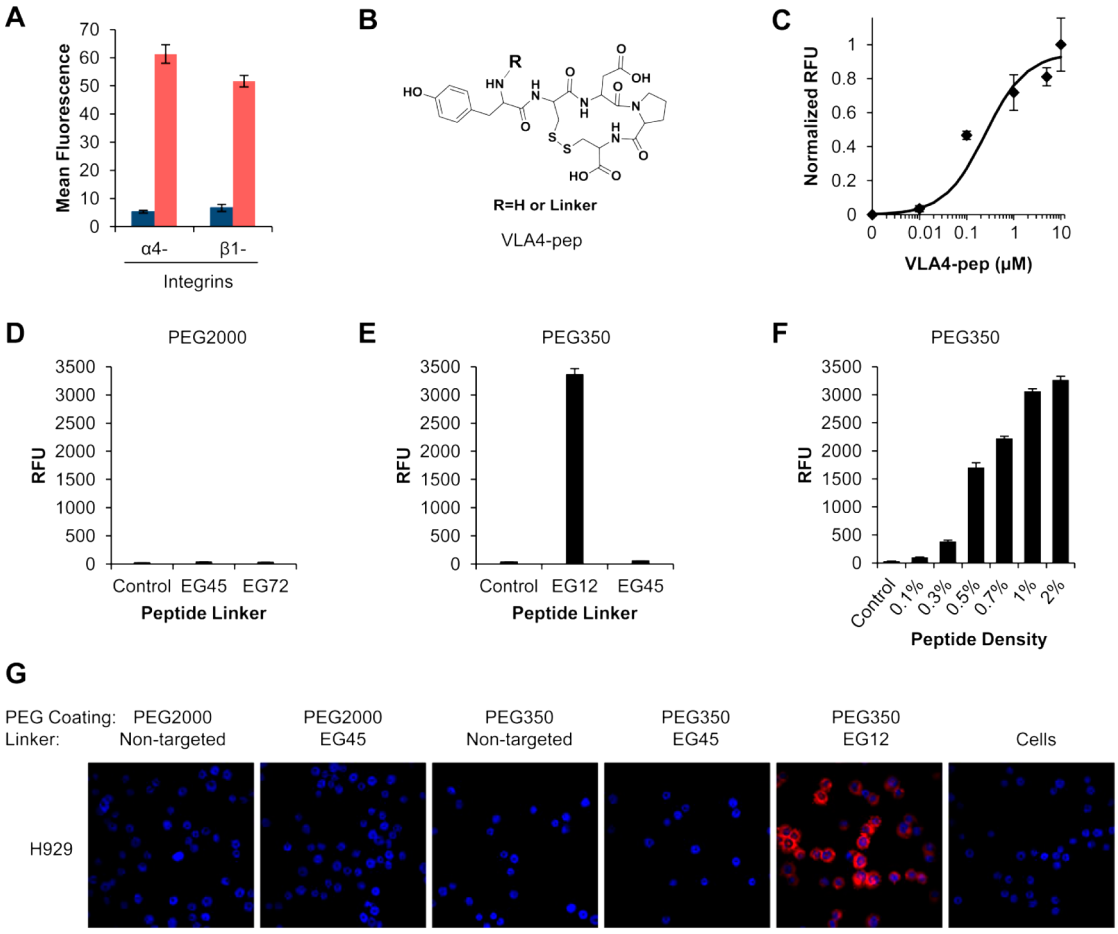

Figure 6. Cellular uptake of VLA-4-targeted liposomes by VLA-4 expressing multiple myeloma cells. (A) NCI-H929 myeloma cells express VLA-4 subunits α_4- and β_1-integrins as determined by flow cytometry. Red columns are primary antibodies and blue columns are isotype controls. (B) Structure of VLA-4-antagonist peptide (VLA4-pep) is shown. (C) Cellular binding assays were performed using fluorescein labeled VLA4-pep and was detected by flow cytometry. Control experiments were done with fluorescein-labeled nonspecific peptide and the background binding was subtracted for each data point. VLA4-pep binds to NCI-H929 with an apparent K_d of ~250 nM. (D) Liposomes composed of PEG2000 coating and either EG45 or EG72 peptide linker were assayed for cellular uptake. (E) Liposomes composed of PEG350 coating and either EG12 or EG45 peptide linker were assayed for cellular uptake. (F) The effect of peptide density on the uptake of VLA4-pep targeted liposomes prepared with PEG350 liposomal coating and EG12 peptide linker is shown. (G) Confocal microscopy images of rhodamine-labeled liposome formulations with the indicated liposomal PEG coating and peptide EG-linker are shown. Non-targeted liposomes were included as controls. Internalization of nanoparticles was determined with a Nikon A1R confocal microscope using a 40× oil lens. Image acquisition was performed by Nikon Elements Ar software.

declined at longer linker lengths, completely diminishing at EG45. Uptake again reached a maximum and a plateau at 1−2% peptide density (95:10:(5-*n*):*n* HSPC:CHOL:PEG350:VLA4-pep-EG12-PA where $n = 0-2$) (Figure 6F). Nanoparticle internalization (95:10:5 HSPC:CHOL:PEGX-DSPE for control liposomes and 95:10:3:2 HSPC:CHOL:PEGX-DSPE:VLA4-pep for targeted liposomes) was also confirmed by confocal microscopy (Figure 6G). Colocalization studies performed with the lysosomal marker Lysotracker Red and fluorescein-labeled nanoparticles (95:10:5 HSPC:CHOL:PEG350 for the control liposome and 95:10:3:2 HSPC:CHOL:PEG350:VLA4-pep-EG12-PA for the targeted liposome) showed significant internalization of the liposomes targeted with the EG12 linker into lysosomes (see Supporting Information, Figure S23).

These results were consistent with the HER2 targeting system validating that the drawn conclusions can be applied broadly to other peptide targeted liposomes and are not disease, receptor, or peptide specific. It is noteworthy that the exact optimal linker length between different model systems may shift slightly depending on the intrinsic chemical properties of each peptide. For example, a peptide sequence with several hydrophobic residues may require a longer EG-linker to help increase its solubility and enhance its accessibility for its target receptor. Specific ligand−receptor interactions may also play a significant role in the optimal EG linker length depending on the depth of the binding pocket on the receptor for that particular peptide, since deeper pockets may require longer linker lengths for maximal targeting. Finally, although same trends were observed both for the VLA-4 and HER2 system regarding the optimal PEG coating, and EG-linker length, VLA-4 targeting was significantly

more efficient than the HER2 targeting for cellular uptake as only 0.3% VLA-4-pep was required to achieve ~10 fold enhancement compared to 2% HER2-pep. This is most probably as a result of differences in the trafficking of the VLA-4 receptors in myeloma cells and HER2 receptors on the breast cancer cells. For this reasoning alone, the VLA-4 targeting system may prove more efficacious for an *in vivo* drug delivery application due to the significantly less peptide density required to achieve comparable uptake to the HER2 system.

CONCLUSIONS

Nanotechnology has been recognized by the National Cancer Institute as a paradigm-changing opportunity with the potential to make significant breakthroughs in various applications including cancer diagnosis and therapy.[59] Ligand-targeted nanoparticles, however, have not consistently delivered successful outcomes.[15−17] One major factor that contributes to the observed inconsistencies is the commonly used synthetic methods to prepare targeted nanoparticles, which result in a heterogeneous surface with variable number of attachments and deactivated binding sites. Another major factor is the differences in the PEG coating of the particles, linkers used to conjugate the targeting ligands, as well as the type of targeting ligands. In this study, we have employed a multifaceted synthetic strategy to prepare ligand-targeted liposomal nanoparticles with high purity and precisely controlled stoichiometry of functionalities to evaluate the role of liposomal PEG coating, peptide EG-linker length, and peptide valency on cellular uptake. Our studies demonstrated that the cellular uptake of nanoparticles can be significantly enhanced by generating liposomes consisting of PEG350 liposomal coating and a shorter peptide linker such as EG12. In particular, our results show that if the peptide linker is shorter than the liposomal PEG coating (*i.e.*, EG6 linker), the peptide is hindered in its ability to bind to the receptor. As the linker length increases and the ligand begins to extend beyond the PEG coating, the peptide efficiently binds to its respective receptor, thereby enabling efficient uptake. In the HER2 overexpressing breast cancer model, EG12 and EG18 peptide linkers, which are 1.5 and 2.25 times longer than the liposomal PEG350 length when linear, enhanced cellular uptake by ~9 fold. As the linker length increased beyond these values, however, the binding of the ligand to the HER2 receptor decreased, returning to background levels at the EG45 (~PEG2000) linker length. These results and conclusions were established in both the HER2-overexpressing breast cancer model and the VLA-4-overexpressing multiple myeloma model demonstrating that our observations are not disease, receptor, or peptide specific. Taken together, the results presented here demonstrate the importance of using the right design elements, such as the appropriate peptide EG-linker length in coordination with the appropriate liposomal PEG coating, and optimal ligand density in efficient cellular uptake of liposomal nanoparticles.

Although, one can argue that the *in vitro* evaluation of nanoparticulate systems may not have direct relevance in *in vivo* applications, as we demonstrated here, without cellular testing, it would be impossible to identify the design features for achieving enhanced cellular uptake. For successful *in vivo* administration, we anticipate several factors to have a combined effect on the therapeutic outcome of targeted liposomal drug delivery systems such as (i) selective targeting of tumors; (ii) uptake of nanoparticles by the tumor cell; (iii) clearance by RES; and (iv) tumor tissue penetration. Evaluation of the overall effect of these parameters on therapeutic outcomes is currently being assessed by incorporating therapeutic agents into our peptide-targeted nanoparticles and studying end points including tumor growth inhibition and systemic toxicity on several mouse models of cancers. In addition, we are analyzing how each of these factors contributes to the overall outcome. The results of the *in vivo* studies may also vary depending on the inherent chemical properties of the selected peptide, expression level, and trafficking of the targeted receptors, as well as the differences in the tumor models used. Additional liposome parameters such as the effect of cholesterol, bulk lipid selection (saturated/unsaturated phospholipids), and chemotherapeutic incorporation and loading techniques may have further implications in targeting efficiency and *in vivo* effectiveness. These studies are currently ongoing in our laboratory. Importantly, the nanoparticle synthetic strategy employed in this study addresses several major hurdles in nanoparticle preparation by providing precise control over the number of functionalities conjugated to each nanoparticle, thereby minimizing particle surface heterogeneity, polydispersity, and batch-to-batch variability in synthesis. In the long run, we predict that this multifaceted synthetic strategy, combined with the identification of the optimal design elements for targeting various cancers, will enable successful applications of ligand-targeted liposomes in medicine.

METHODS

Materials. The list of materials includes *N*-Fmoc-amino acids, NovaPEG Rink amide resin, Wang resin, 2-(1*H*-benzotriazole-1-yl)-1,1,3,3-tetramethyluronium hexafluorophosphate (HBTU), and bovine serum albumin (BSA) from EMD Millipore (Billerica, MA); Fmoc-$(EG)_n$—OH modification reagents from Quanta Biodesign (Powell, OH); palmitic acid, cholesterol, *N*,*N*-diisopropylethylamine (DIEA), trifluoroacetic acid (TFA), triisopropylsilane (TIS), acetonitrile (ACN), 2-propanol, *N*,*N*-dimethylformamide (DMF), and piperidine from Sigma-Aldrich (St. Louis, MO); fluorescein 5-Isothiocyanate (FITC) from Toronto Reseach Chemicals

(Toronto, Canada); secondary goat antihuman fluorescein conjugated antibody from Jackson ImmunoResearch (West Grove, PA); all methoxy PEG-DSPE (PEG-DSPE) lipids, DSPE-PEG2000-NH_2, fluorescein PE, and lissamine rhodamine B PE from Avanti Polar Lipids, Inc. (Alabaster, AL).

Humanized mouse mAb Herceptin was provided by Dr. Rudolph Navari (Indiana University School of Medicine).

Synthesis of Peptides and Peptide−EG−Lipid Conjugates. Ligands were synthesized using Fmoc chemistry on a solid support using Rink amide or Wang resin. Residues were activated with HBTU and DIEA in DMF for 3 min and coupling efficiency was monitored using Kaiser test. The Fmoc protected residues were deprotected with three applications of 20% piperidine in DMF for 3 min each time. The molecules were cleaved from the solid support using 94/2.5/2.5/1 TFA/H_2O/EDT/TIS mixture twice for 30 min each time. We purified the molecules using RP-HPLC on an Agilent (Santa Clara, CA) 1200 series system with a semipreparative Zorbax C18 column or Zorbax C3 column with either acetonitrile or isopropyl alcohol gradients in the mobile phase. We monitored the column eluent with a diode array detector allowing a spectrum from 200 to 400 nm to be analyzed. The purified product was characterized using a Bruker Autoflex III Smartbeam matrix-assisted laser desorption ionization time of flight mass spectrometer (MALDI-TOF-MS, Billerica, MA). Peptide cyclization through disulfide bond formulation was performed in DMF with DIEA under stirring overnight.

Characterization of Liposomes. Particle size was measured using DLS analysis *via* the *90Plus* nanoparticle size analyzer (Brookhaven Instruments Corp., Long Island, NY), using 658 nm light observed at a fixed angle of 90° at 20 °C. Zeta potential was measured using the *ZetaPlus* zeta potential analyzer (Brookhaven Instruments Corp.).

Cell Culture. SK-BR-3 and NCI-H929 cell lines were obtained from American Type Culture Collection (Rockville, MD). BT-474 cells were a generous gift from John Park at the University of California, San Francisco. SK-BR-3 cells were cultured in McCoy's 5A (ATCC) media, while BT-474 and NCI-H929 cell lines were cultured in RPMI 1640 media (Cellgro, Manassas, VA). All lines were supplemented with 10% fetal bovine serum (FBS), 2 mM L-glutamine (Gibco, Carlsbad, CA), 100 U/mL penicillin, and 100 μg/mL streptomycin (Gibco). NCI-H929 cells were supplemented with an additional 10% FBS and 55 μM 2-mercaptoethanol.

HER2 or VLA-4 Expression Analysis and Cell-Based Peptide Binding Assays. For antibody binding assays, cells were incubated with the primary antibody in binding buffer (1.5% BSA in PBS pH 7.4) on ice for 1 h and were washed twice. Fluorescein conjugated secondary antibody was added for 1 h on ice, samples were washed, and analyzed on Guava easyCyte 8HT flow cytometer (Millipore). For cell-based peptide binding assays, cells were incubated with increasing concentrations of fluorescein-conjugated peptides for 2 h on ice. Samples were washed twice and analyzed on Guava easyCyte 8HT flow cytometer.

Liposome Preparation. Liposomes were prepared by dry film hydration as described previously.[60] Briefly, a lipid mixture of chloroform stocks was prepared and dried to form a thin film using nitrogen gas then placed under vacuum overnight to remove residual solvent. The lipid films were hydrated at 65 °C in PBS pH 7.4, gently agitated, and extruded at 65 °C through a 0.1 μm polycarbonate filter. Liposomes all adhered to the following formula 95:10:(5 − *n*):*n*HSPC:CHOL:PEG*X*-DSPE:peptide−EG−lipid conjugate, where *n* was varied between 0 and 5 to control the peptide density and *X* respresents PEG molecular weights, including 350, 550, 750, 1000, or 2000.

***In Vitro* Liposome Uptake and Binding Assays.** A total of 1×10^5 cells/well were plated 24 h prior to each experiment in a 24 well dish. Liposomes were added at 100 μM phospholipid concentration and incubated for 3 h at 37 °C. Fluorescein PE at 0.2% was added as a fluorescent marker to each liposomal formulation. For adherent cells, after incubation, cells were washed three times with PBS, trypsinized, and analyzed *via* flow cytometry. For suspension cells, after incubation, cells were washed three times with PBS and analyzed *via* flow cytometry. For binding assays, adherent cells were scraped from the surface of a confluent dish, placed in growth media, and incubated on ice for 30 min. Liposomes were added at variable concentrations and incubated for 2 h on ice. After incubation, cells were washed three times with PBS and analyzed *via* flow cytometry.

Confocal Microscopy. For breast cancer cells, 1×10^5 cells/well were plated 24 h prior to each experiment onto 12 mm diameter borosilicate glass coverslips in a 24 well dish. Liposomes were added at 100 μM phospholipid concentration and incubated for 3 h at 37 °C. Rhodamine PE at 1% was added as a fluorescent marker to each liposomal formulation. After incubation, cells were washed three times with PBS and fixed with 4 w/w% paraformaldehyde (PFA). Coverslips were mounted on microscope slides with VectaShield antifade/DAPI (Vector Laboratories, Burlingame, CA). For suspension cells, after incubation, cells were washed three times and cytospinned onto slides before fixing and coverslip mounting. For colocalization studies, 1% fluorescein PE was added as a fluorescent marker to each liposomal formulation. After 3 h of liposome incubation, the cells were washed three times with PBS and incubated with 50 nM of Lysotracker Red (Molecular Probes, Carlsbad, CA) for 30 min at 37 °C to allow internalization. Cells were washed three times, fixed in PFA, and mounted on glass slides using Prolong Gold Antifade Reagent (Molecular Probes). Cells were visualized by Nikon A1R confocal microscope with a 40× oil lens (Nikon Instruments, Melville, NY). Image acquisition was performed by Nikon Elements Ar software (Nikon).

Conflict of Interest: The authors declare no competing financial interest.

Acknowledgment. We thank the Notre Dame Integrated Imaging Facility for confocal microscopy, the Center for Environmental Science and Technology for the use of DLS, and the Mass Spectrometry and Proteomics Facility for the use of MALDI-TOF-MS.

Supporting Information Available: Mass spectrometry and product yields of peptide−EG−lipid conjugates, further liposome characterization, and additional imaging and liposomal uptake experiments. This material is available free of charge *via* the Internet at http://pubs.acs.org.

REFERENCES AND NOTES

1. Malam, Y.; Loizidou, M.; Seifalian, A. M. Liposomes and Nanoparticles: Nanosized Vehicles for Drug Delivery in Cancer. *Trends Pharmacol. Sci.* **2009**, *30*, 592–599.
2. Allen, T. M.; Cheng, W. W. K.; Hare, J. I.; Laginha, K. M. Pharmacokinetics and Pharmacodynamics of Lipidic Nano-particles in Cancer. *Anti-Cancer Agents Med. Chem.* **2006**, *6*, 513–523.
3. Sapra, P.; Tyagi, P.; Allen, T. M. Ligand-Targeted Liposomes for Cancer Treatment. *Curr. Drug Delivery* **2005**, *2*, 369–381.
4. Immordino, M. L.; Dosio, F.; Cattel, L. Stealth Liposomes: Review of the Basic Science, Rationale, and Clinical Applications, Existing and Potential. *Int. J. Nanomed.* **2006**, *1*, 297–315.
5. Allen, T. Liposomal Drug Formulations—Rationale for Development and What We Can Expect for the Future. *Drugs* **1998**, *56*, 747–756.
6. Nie, S. Understanding and Overcoming Major Barriers in Cancer Nanomedicine. *Nanomedicine* **2010**, *5*, 523–528.
7. Vega, J.; Ke, S.; Fan, Z.; Wallace, S.; Charsangavej, C.; Li, C. Targeting Doxorubicin to Epidermal Growth Factor Receptors by Site-Specific Conjugation of C225 to Poly-(L-glutamic acid) through a Polyethylene Glycol Spacer. *Pharm. Res.* **2003**, *20*, 826–832.
8. Sofou, S.; Sgouros, G. Antibody-Targeted Liposomes in Cancer Therapy and Imaging. *Expert Opin. Drug Delivery* **2008**, *5*, 189–204.
9. Dubey, P.; Mishra, V.; Jain, S.; Mahor, S.; Vyas, S. Liposomes Modified with Cyclic RGD Peptide for Tumor Targeting. *J. Drug Target.* **2004**, *12*, 257–264.
10. Torchilin, V. Recent Advances with Liposomes as Pharmaceutical Carriers. *Nat. Rev. Drug Discovery* **2005**, *4*, 145–160.
11. Schally, A. V. New Approaches to the Therapy of Various Tumors Based on Peptide Analogues. *Horm. Metab. Res.* **2008**, *40*.

12. Zhao, X.; Li, H.; Lee, R. J. Targeted Drug Delivery *via* Folate Receptors. *Expert Opin. Drug Delivery* **2008**, *5*.
13. Allen, T. Ligand-Targeted Therapeutics in Anticancer Therapy. *Nat. Rev. Cancer* **2002**, *2*, 750–763.
14. Yezhelyev, M. V.; Gao, X.; Xing, Y.; Al-Hajj, A.; Nie, S.; O'Regan, R. M. Emerging Use of Nanoparticles in Diagnosis and Treatment of Breast Cancer. *Lancet Oncol.* **2006**, *7*, 657–667.
15. Sinha, R.; Kim, G. J.; Nie, S.; Shin, D. M. Nanotechnology in Cancer Therapeutics: Bioconjugated Nanoparticles for Drug Delivery. *Mol. Cancer Ther.* **2006**, *5*, 1909–1917.
16. Ferrari, M. Cancer Nanotechnology: Opportunities and Challenges. *Nat. Rev. Cancer* **2005**, *5*, 161–171.
17. Farokhzad, O. C.; Langer, R. Impact of Nanotechnology on Drug Delivery. *ACS Nano* **2009**, *3*, 16–20.
18. Pirollo, K. F.; Chang, E. H. Does a Targeting Ligand Influence Nanoparticle Tumor Localization or Uptake? *Curr. Trends Biotechnol.* **2008**, *26*, 552–558.
19. Bartlett, D. W.; Su, H.; Hildebrandt, I. J.; Weber, W. A.; Davis, M. E. Impact of Tumor-Specific Targeting on the Biodistribution and Efficacy of siRNA Nanoparticles Measured by Multimodality *in Vivo* Imaging. *Proc. Natl. Acad. Sci. U.S.A.* **2007**, *104*, 15549–15554.
20. Kirpotin, D. B.; Drummond, D. C.; Shao, Y.; Shalaby, M. R.; Hong, K.; Nielsen, U. B.; Marks, J. D.; Benz, C. C.; Park, J. W. Antibody Targeting of Long-Circulating Lipidic Nanoparticles Does Not Increase Tumor Localization but Does Increase Internalization in Animal Models. *Cancer Res.* **2006**, *66*, 6732–6740.
21. Garanger, E.; Boturyn, D.; Dumy, P. Tumor Targeting with RGD Peptide Ligands-Design of New Molecular Conjugates for Imaging and Therapy of Cancers. *Anti-Cancer Agents Med. Chem.* **2007**, *7*, 552–558.
22. Hilgenbrink, A.; Low, P. Folate Receptor-Mediated Drug Targeting: From Therapeutics to Diagnostics. *J. Pharm. Sci.* **2005**, *94*, 2135–2146.
23. Xu, L.; Pirollo, K.; Tang, W.; Rait, A.; Chang, E. Transferrin-Liposome-Mediated Systemic p53 Gene Therapy in Combination with Radiation Results in Regression of Human Head and Neck Cancer Xenografts. *Hum. Gene Ther.* **1999**, *10*, 2941–2952.
24. Daniels, T. R.; Delgado, T.; Rodriguez, J. A.; Helguera, G.; Penichet, M. L. The Transferrin Receptor Part I: Biology and Targeting with Cytotoxic Antibodies for the Treatment of Cancer. *Clin. Immunol.* **2006**, *121*, 144–158.
25. Allen, T. M.; Hansen, C.; Martin, F.; Redemann, C.; Yauyoung, A. Liposomes Containing Synthetic Lipid Derivatives of Poly(ethylene glycol) Show Prolonged Circulation Half-Lives *in Vivo*. *Biochim. Biophys. Acta* **1991**, *1066*.
26. Kirpotin, D.; Park, J.; Hong, K.; Zalipsky, S.; Li, W.; Carter, P.; Benz, C.; Papahadjopoulos, D. Sterically Stabilized Anti-HER2 Immunoliposomes: Design and Targeting to Human Breast Cancer Cells *in Vitro*. *Biochemistry* **1997**, *36*, 66–75.
27. Sapra, P.; Allen, T. Ligand-Targeted Liposomal Anticancer Drugs. *Prog. Lipid Res.* **2003**, *42*, 439–462.
28. Gabizon, A.; Horowitz, A. T.; Goren, D.; Tzemach, D.; Shmeeda, H.; Zalipsky, S. *In Vivo* Fate of Folate-Targeted Polyethylene−Glycol Liposomes in Tumor-Bearing Mice. *Clin. Cancer Res.* **2003**, *9*.
29. Yamada, A.; Taniguchi, Y.; Kawano, K.; Honda, T.; Hattori, Y.; Maitani, Y. Design of Folate-Linked Liposomal Doxorubicin to its Antitumor Effect in Mice. *Clin. Cancer Res.* **2008**, *14*.
30. Allen, C.; Dos Santos, N.; Gallagher, R.; Chiu, G.; Shu, Y.; Li, W.; Johnstone, S.; Janoff, A.; Mayer, L.; Webb, M.; *et al.* Controlling the Physical Behavior and Biological Performance of Liposome Formulations through Use of Surface Grafted Poly(ethylene glycol). *Biosci. Rep.* **2002**, *22*, 225–250.
31. Dos Santos, N.; Allen, C.; Doppen, A.; Anantha, M.; Cox, K. A. K.; Gallagher, R. C.; Karlsson, G.; Edwards, K.; Kenner, G.; Samuels, L.; *et al.* Influence of Poly(ethylene glycol) Grafting Density and Polymer Length On Liposomes: Relating Plasma Circulation Lifetimes to Protein Binding. *Biochim. Biophys. Acta, Biomembr.* **2007**, *1768*, 1367–1377.
32. Tirosh, O.; Barenholz, Y.; Katzhendler, J.; Priev, A. Hydration of Polyethylene Glycol-Grafted Liposomes. *Biophys. J.* **1998**, *74*, 1371–1379.
33. Barenholz, Y. Liposome Application: Problems and Prospects. *Curr. Opin. Colloid Interface Sci.* **2001**, *6*, 66–77.
34. Noble, C.; Kirpotin, D.; Hayes, M.; Mamot, C.; Hong, K.; Park, J.; Benz, C.; Marks, J.; Drummond, D. Development of Ligand-Targeted Liposomes for Cancer Therapy. *Expert Opin. Ther. Targets* **2004**, *8*, 335–353.
35. Lee, T.; Lin, C.; Kuo, S.; Chang, D.; Wu, H. Peptide-Mediated Targeting to Tumor Blood Vessels of Lung Cancer for Drug Delivery. *Cancer Res.* **2007**, *67*, 10958–10965.
36. Marty, C.; Meylan, C.; Schott, H.; Ballmer-Hofer, K.; Schwendener, R. A. Enhanced Heparan Sulfate Proteoglycan-Mediated Uptake of Cell-Penetrating Peptide-Modified Liposomes. *Cell. Mol. Life Sci.* **2004**, *61*.
37. Torchilin, V. P.; Rammohan, R.; Weissig, V.; Levchenko, T. S. TAT Peptide on the Surface of Liposomes Affords Their Efficient Intracellular Delivery Even at Low Temperature and in the Presence of Metabolic Inhibitors. *Proc. Natl. Acad. Sci. U.S.A.* **2001**, *98*, 8786–8791.
38. Hansen, C.; Kao, G.; Moase, E.; Zalipsky, S.; Allen, T. Attachment of Antibodies to Sterically Stabilized Liposomes—Evaluation, Comparison and Optimization of Coupling Procedures. *Biochim. Biophys. Acta, Biomembr.* **1995**, *1239*, 133–144.
39. Veronese, F. Peptide and Protein PEGylation: A Review of Problems and Solutions. *Biomaterials* **2001**, *22*, 405–417.
40. Pasut, G.; Guiotto, A.; Veronese, F. Protein, Peptide and Nonpeptide Drug PEGylation for Therapeutic Application. *Expert Opin. Ther. Pat.* **2004**, *14*, 859–894.
41. Nobs, L.; Buchegger, F.; Gurny, R.; Allemann, E. Current Methods for Attaching Targeting Ligands to Liposomes and Nanoparticles. *J. Pharm. Sci.* **2004**, *93*, 1980–1992.
42. Slamon, D. J.; Godolphin, W.; Jones, L. A.; Holt, J. A.; Wong, S. G.; Keith, D. E.; Levin, W. J.; Stuart, S. G.; Udove, J.; Ullrich, A.; *et al.* Studies of the Her-2/neu Proto-Oncogene in Human-Breast and Ovarian-Cancer. *Science* **1989**, *244*.
43. Slamon, D. J.; Clark, G. M.; Wong, S. G.; Levin, W. J.; Ullrich, A.; Mcguire, W. L. Human-Breast Cancer—Correlation of Relapse and Survival with Amplification of the Her-2 Neu Oncogene. *Science* **1987**, *235*.
44. Lewis, G. D.; Figari, I.; Fendly, B.; Wong, W. L.; Carter, P.; Gorman, C.; Shepard, H. M. Differential Responses of Human Tumor-Cell Lines to Anti-P185(her2) Monoclonal-Antibodies. *Cancer Immunol. Immunother.* **1993**, *37*.
45. Arap, W.; Pasqualini, R.; Ruoslahti, E. Cancer Treatment by Targeted Drug Delivery to Tumor Vasculature in a Mouse Model. *Science* **1998**, *279*, 377–380.
46. Forssen, E.; Willis, M. Ligand-Targeted Liposomes. *Adv. Drug Delivery Rev.* **1998**, *29*, 249–271.
47. Ellerby, H.; Arap, W.; Ellerby, L.; Kain, R.; Andrusiak, R.; Del Rio, G.; Krajewski, S.; Lombardo, C.; Rao, R.; Ruoslahti, E.; *et al.* Anti-cancer Activity of Targeted Pro-Apoptotic Peptides. *Nat. Med.* **1999**, *5*, 1032–1038.
48. Schiffelers, R.; Koning, G.; ten Hagen, T.; Fens, M.; Schraa, A.; Janssen, A.; Kok, R.; Molema, G.; Storm, G. Anti-Tumor Efficacy of Tumor Vasculature-Targeted Liposomal Doxorubicin. *J. Controlled Release* **2003**, *91*, 115–122.
49. Reubi, J. Peptide Receptors as Molecular Targets for Cancer Diagnosis and Therapy. *Endocr. Rev.* **2003**, *24*, 389–427.
50. Owen, R. M.; Carlson, C. B.; Xu, J. W.; Mowery, P.; Fasella, E.; Kiessling, L. L. Bifunctional Ligands That Target Cells Displaying the Alpha(v)beta(3) Integrin. *ChemBioChem* **2007**, *8*, 68–82.
51. Mammen, M.; Choi, S. K.; Whitesides, G. M. Polyvalent Interactions in Biological Systems: Implications for Design and Use of Multivalent Ligands and Inhibitors. *Angew. Chem., Int. Ed.* **1998**, *37*, 2755–2794.
52. Berezov, A.; Zhang, H. T.; Greene, M. I.; Murali, R. Disabling ErbB Receptors with Rationally Designed Exocyclic Mimetics of Antibodies: Structure−Function Analysis. *J. Med. Chem.* **2001**, *44*, 2565–2574.
53. Gabizon, A.; Horowitz, A.; Goren, D.; Tzemach, D.; Mandelbaum-Shavit, F.; Qazen, M.; Zalipsky, S. Targeting Folate Receptor with Folate Linked to Extremities of Poly-(ethylene glycol)−Grafted Liposomes: *in Vitro* Studies. *Bioconjugate Chem.* **1999**, *10*, 289–298.

54. Xia, W.; Low, P. S. Folate-Targeted Therapies for Cancer. *J. Med. Chem.* **2010**, *53*, 6811–6824.
55. Lin, K.; Castro, A. Very Late Antigen 4 (VLA4) Antagonists as Anti-inflammatory Agents. *Curr. Opin. Chem. Biol.* **1998**, *2*, 453–457.
56. Singh, J.; Adams, S.; Carter, M.; Cuervo, H.; Lee, W.; Lobb, R.; Pepinsky, R.; Petter, R.; Scott, D. Rational Design of Potent and Selective VLA-4 Inhibitors and Their Utility in the Treatment of Asthma. *Curr. Top. Med. Chem.* **2004**, *4*, 1497–1507.
57. Jackson, D.; Quan, C.; Artis, D.; Rawson, T.; Blackburn, B.; Struble, M.; Fitzgerald, G.; Chan, K.; Mullins, S.; Burnier, J.; *et al*. Potent Alpha 4 Beta 1 Peptide Antagonists as Potential Anti-inflammatory Agents. *J. Med. Chem.* **1997**, *40*, 3359–3368.
58. Kiziltepe, T.; Ashley, J. D.; Stefanick, J. F.; Qi, Y. M.; Alves, N. J.; Handlogten, M. W.; Suckow, M. A.; Navari, R. M.; Bilgicer, B. Rationally Engineered Nanoparticles Target Multiple Myeloma Cells, Overcome Cell-Adhesion-Mediated Drug Resistance, and Show Enhanced Efficacy *in Vivo*. *Blood Cancer J.* **2012**, *2*, e64.
59. Roco, M. C. The Long View of Nanotechnology Development: The National Nanotechnology Initiative at 10 Years. *J. Nanopart. Res.* **2011**, *13*, 427–445.
60. Olson, F.; Hunt, C. A.; Szoka, F. C.; Vail, W. J.; Papahadjopoulos, D. Preparation of Liposomes of Defined Size Distribution by Extrusion through Polycarbonate Membranes. *Biochim. Biophys. Acta* **1979**, 557.